

Positive-Pion Production by 160-MeV Protons on  $^{90}\text{Zr}$  and  $^{208}\text{Pb}$ 

R. D. Bent, P. T. Debevec,<sup>(a)</sup> P. H. Pile, R. E. Pollock, R. E. Marrs, and M. C. Green  
*Indiana University Cyclotron Facility, Bloomington, Indiana 47401*

(Received 16 December 1977)

Angular distributions for the reactions  $^{90}\text{Zr}(p,\pi^+)^{91}\text{Zr}(\text{g.s.})$  and  $^{208}\text{Pb}(p,\pi^+)^{209}\text{Pb}(0.0, 0.78, \text{ and } 1.41 \text{ MeV})$  at 160 MeV have been measured from 25 to 155 deg using a quadrupole-dipole-dipole-multipole magnetic spectrograph. The  $^{90}\text{Zr}$  angular distribution has a shallow minimum at about 80 deg; the  $^{208}\text{Pb}$  angular distributions have minima at more forward angles and rise markedly in the backward hemisphere. The  $(p,\pi^+)$  cross sections observed in this mass region depend weakly on target mass and angular momentum transfer.

Earlier work on pion production in proton-nucleus collisions has generated considerable interest in the mechanism of  $(p,\pi)$  reactions near threshold and in the use of these reactions to study nuclear structure in new kinematical regions. In the pioneering experiments near threshold reported by Dahlgren *et al.*<sup>1</sup> and LeBorne and co-workers,<sup>2</sup> charged-pion production on targets ranging from  $^9\text{Be}$  to  $^{40}\text{Ca}$  was studied. We report here on the first measurements of charged-pion production near threshold in proton collisions with heavy nuclei. This work complements recent near-threshold measurements<sup>3</sup> of the  $(p,\pi^0)$  reaction on targets ranging from  $^{10}\text{B}$  to  $^{208}\text{Pb}$ .

The present measurements were made at the Indiana University Cyclotron Facility (IUCF) with the quadrupole-dipole-dipole-multipole magnetic spectrograph shown in Fig. 1. This spectrograph is used primarily for heavy-charged-particle spectroscopy at IUCF and is much larger than necessary for pion experiments. It has a maximum solid angle of 3.4 msr, a momentum range in the focal plane of 3%, and a dispersion of (15 cm)/(% of momentum range). The focal plane is 45 cm long with a  $44^\circ$  orientation with respect to the central ray. The flight path from the target to the last detector is 6.8 m, corresponding to 84% pion decay for 15-MeV pions. The number of decay muons reaching the detectors and mistakenly identified as pions was estimated from geometrical constraints to be less than a few percent of the 15-MeV pion yield and has been neglected.

The detector array consists of a helical multiwire proportional chamber at the position of the spectrograph's horizontal focal plane, followed by 0.32-cm- (or 0.64-cm-) and 1.27-cm-thick scintillators separated by a distance of 30 cm and a third 1.27-cm-thick scintillator. The three scintillators were located at the spectrograph's isochronous angle. For low-energy pions which

stopped in the second scintillator, the third scintillator was used to veto background due to high-energy protons; for more energetic pions it provided a third  $\Delta E$  signal. Measurements were made of the pion's positions in the helix and in the second scintillator (by timing from both ends), the time of flight between the first two scintillators, and the energy losses in all three scintillators. Pions were identified on-line by multiparameter computer analysis of these seven measured quantities. Event-mode data were also recorded on magnetic tape so that the data could be reanalyzed off-line with refined conditions placed on the various parameters. The

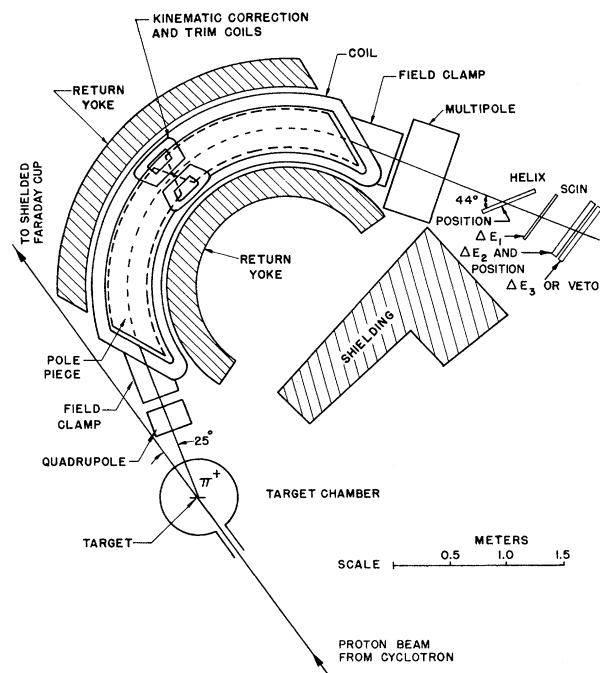


FIG. 1. Experimental arrangement showing the target chamber, quadrupole-dipole-dipole-multipole magnetic spectrograph, and focal-plane detector array.

singles counting rate in the second scintillator with 100 nA of beam current on the target was of the order of  $10^5$ /sec. Pion event rates ranged from thirty counts per minute for  $^{10}\text{B}$  (which was used for setup) to a few counts per minute for  $^{90}\text{Zr}$  and  $^{208}\text{Pb}$  targets. A background level of  $\sim 1$  nb/sr was achieved.

Examples of the data are shown in Fig. 2. The events displayed in these two-dimensional energy planes were required by the computer to fall along a straight line in the plane of helix position versus scintillator position, corresponding to particles transmitted by the spectrograph, and also to satisfy the two time-of-flight conditions for pions. The Pb spectrum, which was taken at a pion laboratory angle of 25 deg with a 129.5-mg/cm<sup>2</sup> target, shows thirty pion events and was obtained in a 3.5-h run with an average beam current of 50 nA. The Zr spectrum contains forty pion events which were accumulated in a 104-min run at  $\theta_\pi(\text{lab}) = 110$  deg with a 77.5-mg/cm<sup>2</sup> target and an average beam current of 93 nA. The thickness of the first scintillator was 0.32 cm for the Pb run and 0.64 cm for the Zr run.

Cross sections extracted from data such as those shown in Fig. 2 are plotted in Fig. 3. The average beam current during these angular-dis-

tribution measurements was 140 nA. Beam currents as high as 400 nA were used; however, usually the maximum current was limited to 300 nA either by the cyclotron performance or by the maximum tolerable singles counting rates in the detectors. Typically, approximately 100 min were required to obtain fifty pion events at each angle. The error bars indicate relative errors, which are due mainly to counting statistics. The absolute cross sections are believed to be accurate to about 20%.

One purpose of these experiments was to extend to heavy nuclei the experimental knowledge of the  $A$  dependence of the pion production process near threshold. At higher energies the total cross sections for positive-pion production are known to increase with increasing target mass. For example, Cochran *et al.*<sup>4</sup> using 730-MeV protons have shown that beyond  $^{12}\text{C}$ ,  $\sigma_T(p, \pi^+) \equiv \int (d^2\sigma/d\Omega dE) d\Omega dE$  is proportional to  $Z^{1/3}$ . This result is expected if absorption effects are important and the reaction occurs mainly on a surface ring.<sup>5</sup> In recent inclusive experiments at IUCF at 143 and 151 MeV bombarding energies,

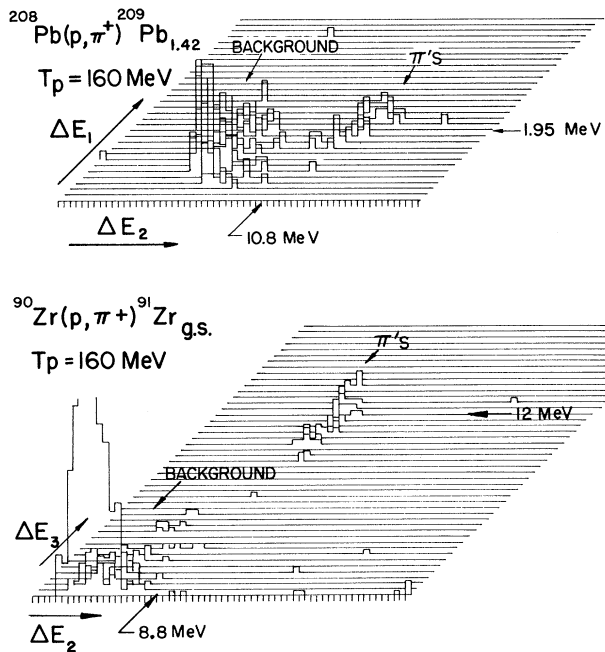


FIG. 2. Examples of pulse-height spectra obtained in the plastic scintillators with cuts on the cyclotron-rf- $\Delta E_1$  time of flight,  $\Delta E_1$ - $\Delta E_2$  time of flight, and helix- $\Delta E_2$  position correlation.

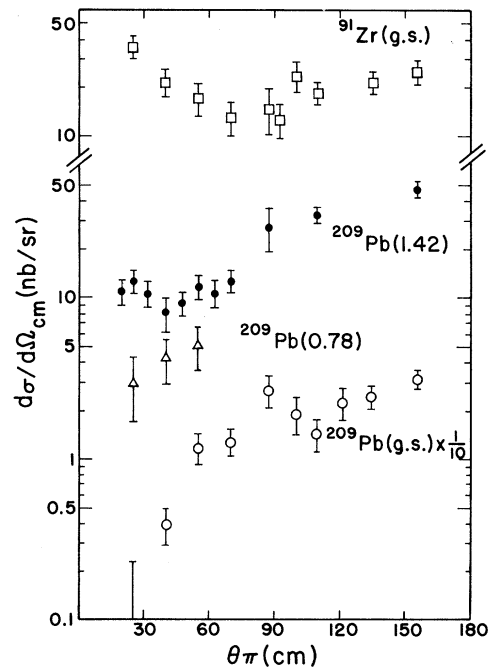


FIG. 3. Angular distribution of pions from the reactions  $^{90}\text{Zr}(p, \pi^+)^{91}\text{Zr}(\text{g.s.})$  and  $^{208}\text{Pb}(p, \pi^+)^{209}\text{Pb}(\text{g.s.}, 0.78, 1.42 \text{ MeV})$  at 160-MeV bombarding energy. The  $^{209}\text{Pb}(\text{g.s.})$  data are displaced downward one decade for display purposes.

Bacher *et al.*<sup>3</sup> have found that the yield of neutral pions is approximately proportional to  $A^{0.47}$  and  $A^{0.43}$ , respectively. The total  $(p, \pi^+)$  cross sections to *discrete nuclear states* obtained from Fig. 3 are listed in Table I, together with those obtained at IUCF for some lighter targets.<sup>6</sup> The pronounced decrease in observed total cross section with increasing target mass is not primarily due to Coulomb effects for these pion energies, which are in each case well above the classical Coulomb barrier.

The  $(p, \pi)$  reaction is a high-momentum-transfer reaction. Consequently, it is reasonable to suppose that it will favor high angular momentum transfer. This conjecture is consistent with fragmentary data of LeBornec and co-workers on *sd*-shell nuclei<sup>7</sup> and distorted-wave Born approximation calculations in the pionic stripping model. Uncertainties in the effective operator for pion production, the pion-nucleus optical potential, and nuclear structure effects make this conjecture far from certain. The  $^{208}\text{Pb}(p, \pi^+)$  reaction to low-lying states of  $^{209}\text{Pb}$ , whose single-particle purities are well established from low-momentum-transfer single-nucleon stripping reactions, was selected as a favorable case for studying the sensitivity of the  $(p, \pi^+)$  reaction to angular momentum transfer. The differential cross sections for exciting the ground ( $g_{9/2}$ ), 0.78-MeV ( $i_{11/2}$ ), and 1.42-MeV ( $j_{15/2}$ ) states of  $^{209}\text{Pb}$  are shown in Fig. 3. The total cross section to the 1.42-MeV state is about 50% larger than that to the ground state. The 1.42- and 1.566-MeV states would not have been resolved in the present experiments, and so part of the yield to this region of excitation in  $^{209}\text{Pb}$  may have been due to excitation of the 1.566-MeV ( $d_{5/2}$ ) state. In the stripping model, transitions to the ground, 0.78-, 1.42-, and 1.56-MeV states involve  $l_n = 4, 6, 7,$  and 2, respectively. Comparing to a classical

TABLE I. Total integrated  $(p, \pi^+)$  cross sections derived from the differential cross sections of Fig. 3 and similar unpublished data (see Ref. 6) for  $^{10}\text{B}$  and  $^{40}\text{Ca}$  targets.

Reaction	$T_p$ (lab) (MeV)	$T_\pi$ (c.m.) (MeV)	$\sigma_{\text{total}}$ ( $\mu\text{b}$ )
$^{10}\text{B}(p, \pi^+)^{11}\text{B}_{g.s.}$	166	20.0	$2.50 \pm 0.04$
$^{40}\text{Ca}(p, \pi^+)^{41}\text{Ca}_{g.s.}$	154	17.4	$0.68 \pm 0.03$
$^{90}\text{Zr}(p, \pi^+)^{91}\text{Zr}_{g.s.}$	160	24.4	$0.24 \pm 0.02$
$^{208}\text{Pb}(p, \pi^+)^{209}\text{Pb}_{g.s.}$	160	22.2	$0.21 \pm 0.02$
$^{208}\text{Pb}(p, \pi^+)^{209}\text{Pb}_{1.4}$	160	20.8	$0.32 \pm 0.02$

angular momentum transfer at the nuclear surface of  $|\vec{k}_p - \vec{k}_\pi|R \sim 19$ , we see that this reaction is severely mismatched. The experimental data suggest an angular-momentum-transfer dependence of the cross section which is not stronger than linear.

The small total cross sections reported here for the heavy targets as well as the backward peaking for the case of lead may be due to angular momentum matching and absorption effects. In these experiments both the pion and the proton reduced wavelengths are smaller than the radius of a heavy nucleus, so that a semiclassical model may have some validity. In a semiclassical picture, angular momentum conservation would require an impact parameter much smaller than the radius of a heavy nucleus. For nuclear radii larger than the mean free path of both the proton and the pion, production on a localized region of the backward hemisphere could be favored and production at forward angles reduced by pion absorption. If this picture is valid, the transition from forward peaking for lighter targets to backward peaking for lead may provide useful information on the strength of low-energy pion-absorption effects in nuclear matter. Detailed calculations which take into account both nuclear structure and distortions will be required in order to obtain a fuller understanding of the present data.

This work was supported by the National Science Foundation.

(a) Present address: Department of Physics, University of Illinois, Urbana, Ill. 61801.

<sup>1</sup>S. Dahlgren, P. Grafström, B. Höistad, and A. Åsberg, Nucl. Phys. **A227**, 245 (1974), and references therein.

<sup>2</sup>Y. LeBornec, B. Tatischeff, L. Bimbot, I. Brissaud, J. P. Garron, H. D. Holmgren, F. Reide, and N. Willis, Phys. Lett. **49B**, 434 (1974); Y. LeBornec, B. Tatischeff, L. Bimbot, I. Brissaud, H. D. Holmgren, J. Källne, F. Reide, and N. Willis, Phys. Lett. **61B**, 47 (1976).

<sup>3</sup>A. D. Bacher, P. T. Debevec, G. T. Emery, M. A. Pickar, K. Gotow, and D. A. Jenkins, Bull. Am. Phys. Soc. **21**, 983 (1976), and Indiana University Cyclotron Facility Technical and Scientific Report, November 1975–January 1977 (unpublished), p. 31.

<sup>4</sup>D. R. F. Cochran, P. N. Dean, P. A. M. Gram, E. A. Knapp, E. R. Martin, D. E. Nagle, R. B. Perkins, W. J. Shlaer, H. A. Thiessen, and E. D. Theriot, Phys. Rev. **D 6**, 3085 (1972).

<sup>5</sup>M. M. Sternheim and R. R. Silbar, Phys. Rev. D **6**, 3117 (1972); R. R. Silbar and M. M. Sternheim, Phys. Rev. C **8**, 492 (1973).

<sup>6</sup>R. E. Pollock, R. D. Bent, P. H. Pile, P. T. Debevec, R. E. Marrs, and M. C. Green, Bull. Am. Phys. Soc. **22**, 1006 (1977), and to be published.

<sup>7</sup>Y. LeBornec, B. Tatischeff, L. Bimbot, I. Brissaud, H. D. Holmgren, J. Källne, F. Reide, and N. Willis, in *Meson-Nuclear Physics—1976*, AIP Conference Proceedings No. 33, edited by P. D. Barnes, R. A. Eisenstein, and L. S. Kisslinger (American Institute of Physics, New York, 1976), p. 260.

## Off-Shell Ambiguities and Phenomenological Pion-Nucleus Potentials

Kwang-Bock Yoo and Morton M. Sternheim

*Department of Physics and Astronomy, University of Massachusetts, Amherst, Massachusetts 01003*

(Received 16 December 1977)

The pionic wave functions obtained by fitting phenomenological optical potentials to elastic-scattering data are found to be dependent on the assumed off-shell extrapolation of the  $\pi N$  amplitude. Using data from low-lying excited states or employing finite range potentials does not eliminate the ambiguities.

Considerable effort has been devoted to understanding the pion-nucleus interaction well enough to employ pions effectively as nuclear probes.<sup>1</sup> One aspect which has had substantial attention is the effect of the off-shell behavior of the  $\pi N$  scattering amplitude on *derived* pion-nucleus optical potentials. For example, it has been noted that the Kisslinger and Laplacian forms of the optical model, which are derived using  $\pi N$   $p$ -wave amplitudes which are equal on shell, give quite different differential elastic<sup>2</sup> and total<sup>3</sup> cross sections, as well as pionic-atom<sup>4</sup> level shifts and widths. Here we show that analogous ambiguities occur also with *phenomenological* potentials fitted to the low-energy elastic-scattering data. These ambiguities are not eliminated by considering inelastic data or by using finite-range interactions.

Although the problems are similar for other energies and nuclei, we focus on 50-MeV  $\pi^+C$  scattering. In the experimental paper of Dytman *et al.*,<sup>5</sup> Kisslinger-model parameters were adjusted to fit the elastic data. These parameters were then used as inputs to a distorted-wave impulse-approximation (DWIA) code, yielding fair agreement with the data for the  $2^+$  and  $3^-$  states. These results suggest that the elastic and inelastic data may together define a potential fairly well, but this is not so, as we see below. Furthermore, Dytman *et al.* found good elastic fits only if a small unitarity violation was permitted. This problem can also be avoided.

To explore the dependence on the off-shell  $\pi N$  amplitude, we write the spin-isospin averaged amplitude as

$$(\vec{k}' | t | \vec{k}) = a_0 k_0^2 + a_1 \vec{k} \cdot \vec{k}' = a_0 k_0^2 + a_1 (1 - \lambda) \vec{k} \cdot \vec{k}' + \frac{1}{2} a_1 \lambda (k^2 + k'^2 - q^2). \quad (1)$$

Here  $\vec{q} = \vec{k}' - \vec{k}$  and  $\vec{k}_0$  is the incident momentum. With  $k^2 \simeq k'^2 \simeq k_0^2$ , to lowest order in the nuclear density  $\rho$  the optical potential is  $(\vec{k}' | V_\lambda | \vec{k}) = A t \rho(q)$ , or

$$V_\lambda(r) \simeq b_0 k_0^2 \rho(r) + b_1 [(1 - \lambda) \vec{p} \cdot \rho \vec{p} + \lambda (k_0^2 + \frac{1}{2} \nabla^2) \rho]. \quad (2)$$

When  $\lambda = 0$  (1), this is the Kisslinger (Laplacian) model. Thus we have a family of potentials with varied, albeit unrealistic, off-shell extrapolations.

Using  $b$ 's obtained from the experimental free- $\pi N$  phase shifts, we find that the pionic wave functions and hence the calculated elastic<sup>6</sup> and inelastic<sup>7</sup> differential and total cross sections depend strongly on the off-shell parameter,  $\lambda$  (Fig. 1). Surprisingly, the off-shell sensitivity is greater here than at higher energies, although the  $\pi N$  forces are relatively weak at 50 MeV. What is

happening, as we see below, is that the Kisslinger term proportional to  $1 - \lambda$  gives large and totally unreliable contributions from high-momentum components of the wave function. Closer to the (3, 3) resonance, the greater nuclear opacity reduces the model dependence.

Even though the predictions for a given set of  $b$ 's depend on the off-shell behavior, one might suppose that optical models fitted to the elastic data would be approximately equivalent. To study